JOURNAL OF APPLIED ELECTROCHEMISTRY **26** (1996) 1169–1177

Impedance study of the passive film on stainless steel 304 in pH 8 carbonate solution

M. DROGOWSKA, H. MÉNARD, A. LASIA

Département de Chimie, Université de Sherbrooke, Sherbrooke, Québec, Canada J1K 2R1

L. BROSSARD

Institut de recherche d'Hydro-Québec (IREQ), Varennes, Québec, Canada J3X 1S1

Received 31 August 1995; revised 8 March 1996

The effects of applied d.c. potential and polarization time on the passivation of stainless steel 304 (SS304) were investigated in deaerated 1 M $NaHCO_3$ aqueous solutions at pH 8. Electrochemical impedance spectroscopy was used in conjunction with a rotating disc electrode. The data were analysed by considering an equivalent circuit. The changes in impedance parameters at applied d.c. potential signal changes in the properties of passive films on SS304 and allow to distinguish the parameters at low potential (−0.6 to 0.3 V vs SCE) from a different one at high potential (0.5 to 0.8 V vs SCE). The oxidation reactions were controlled by both charge transfer and mass transfer processes. Diffusional resistance was high for both passive films and was considered to represent the resistance to movement of ions or vacancies through the surface layer of oxide films. It is deduced that the passive film present in the low potential region is partially dissolved at 0.4 V vs SCE and that a new passive film is formed in the higher potential region. The equivalent circuit used to obtain the best fit and the fitting parameters was dependent on the electrode potential and the polarization time. The reproducibility of the impedance spectra at constant potentials demonstrate that the passive film formation is highly irreversible process. No traces of localized corrosion were detected but, for a high potential and long polarization time, the electrode surface coloration to a uniform gold colour confirms the film thickening.

1. Introduction

Stainless steel passivity is of practical importance for corrosion resistance, since the presence of passive films reduces the corrosion rate. The effect of passive films formed in near-neutral solutions on the electrooxidation process of stainless steel is a complex phenomenon because the structure and composition of the film formed may depend on a large number of variables, for example, the pretreatment and composition of the metal surface, the electrode potential, the polarization time, the environment chemistry, temperature, etc.

Recently, it was shown [1] that the properties of the passive film formed on a stainless steel 304 (SS304) electrode in $NaHCO_3$ solutions depend on the applied potential. The low potential passive film (< 0.4 V) is linked to a heterogeneous Cr-rich composition, while at higher potentials (> 0.4 V) it was deduced that a γ-Fe_2O_3 rich film is responsible for SS304 surface passivation. The complex film structure with intermediate non-stoichiometric oxides have been postulated.

Electrochemical impedance spectroscopy (EIS) has achieved considerable importance as an *in situ* technique for studying the electronic properties of anodically formed passive films [2–15, 44–46]. However, usually more than one equivalent circuit can approximate the experimental data and great care must therefore be exercised when trying to use equivalent circuit to explain surface oxidation reactions.

Metal surfaces are usually heterogeneous. This heterogeneity may arise from surface roughness or interfacial phenomena [19] and causes anomalous frequency dispersion of interfacial properties (such as capacitance or impedance). In such cases, to fit the data to an equivalent circuit model containing, a constant phase element (CPE) should be used. Its impedance, Z_{CPE}, is described [16] as

$$Z_{CPE} = 1/T(j\omega)^{\alpha} \quad (1)$$

where ω is the angular frequency in rad s^{-1} and T a capacitance parameter. When used instead of the double layer capacitance, Z_{CPE} causes a rotation of the centre of the capacitive semicircle below the real axis by a frequency independent constant phase angle $\phi = (1 - \alpha)\pi/2$. The value of angle ϕ can vary between 0° for a perfect capacitor ($\alpha = 1$) and 90° for a perfect resistor ($\alpha = 0$). A value of ϕ between 10° and 20° would represent a somewhat leaky capacitor and is generally attributed to the presence of heterogeneities both laterally and within the depth of the passive film. Although Z_{CPE} has been used extensively to model rough surfaces [17–20], and oxide films formation [45, 46], it has not been universally embraced by corrosion scientists. Jüttner [21] discussed the usefulness of Z_{CPE} for corrosion processes on inhomogeneous

0021-891X

surfaces, while Bardwell and McKubre [3] used it to obtain a better fit for experimental data on anodic film on zirconium in a neutral solution.

The present investigation shows that EIS is a suitable technique for characterization of passive films formed on 304 stainless steel in a carbonate solution at pH 8. Special attention is given to the effects of applied potential and polarization time. This work represents the continuation of earlier d.c. measurements for the same system [1].

2. Experimental details

The study was made using austenitic stainless steel 304 (SS304) with the following chemical composition (% in weight): C 0.009, Mn 1.67, P 0.034, S 0.020, Si 0.51, Cu 0.35, Ni 8.2, Cr 19.4, V 0.07, Mo 0.30, Co 0.14, Sn 0.018, Al 0.006, Ti 0.006, Nb 0.033. The stainless steel was machined in the shape of a cylinder and one end of the cylinder was set in a Kel-F holder to form the working rotating disc electrode. The exposed surface area was 1 cm^2. The electrode was mechanically polished with an alumina suspension to mirror finish and rinsed with distilled water. The electrode surface was examined by a Bausch & Lomb optical microscope (70×) before and after the experiments. At the beginning of each experiment, the electrode was immersed in the solution with the potentiostat setting at −0.9 V and cathodically polarized for 60 s to remove some of the surface oxides. A rotation speed of 1000 rpm was used. The auxiliary electrode was a platinum grid separated from the main compartment by a Nafion® membrane. A saturated calomel electrode (SCE) connected to the cell by a bridge with a Luggin capillary served as the reference electrode. All potentials quoted in the paper are referred to this electrode.

The solution used was 1 M $NaHCO_3$ prepared from analytical grade materials (BDH) and deionized water. The pH value was 8, adjusted by adding NaOH. The cell capacity was ~ 600 ml, which ensured that the buildup of dissolved ions in the bulk of the solution during the course of an experiment was negligible. All solutions were deaerated with high-purity nitrogen before each experiment and purged continuously during the measurements. The experiments were carried out at room temperature.

The impedance measurements were performed in potentiostatic mode using a PAR 273A galvanostat–potentionstat, a PAR 5210 lock-in amplifier for the measurements from 20 kHz to 5 Hz, and a fast Fourier transform (FFT) technique for frequencies of 10 Hz to 1 mHz. Fifteen frequencies per decade were scanned using a sinusoidal potential amplitude of 10 mV peak-to-peak. The real (Z') and imaginary (Z'') components obtained experimentally were analysed using a modified complex nonlinear least-squares (CNLS) program [22] from which the parameters were determined.

3. Results and discussion

The electrochemical behaviour of SS304 in the 1 M $NaHCO_3$ solution is illustrated by the voltammogram in Fig. 1 (second and third cycles). The voltammograms became identical after a first cycle. A wide passive region at low anodic potentials (−0.8 to 0.3 V) is followed by electrode activation at ~ 0.4 V and a second passive region at high positive potentials (0.7 to 0.85 V) before oxygen evolution. The anodic electrode activity increased as the electrode was scanned to more negative potentials but the passive film was not completely reduced, regardless of the cathodic potential supplied. A detailed analysis of these voltammograms has been given elsewhere [1].

As shown below, the impedance characteristics observed for anodic films on an SS304 electrode in a 1 M $NaHCO_3$ solution were found to depend on applied oxidation potential and polarization time.

3.1. *Effect of d.c. potential*

For hydrogen or oxygen evolution, the impedance spectrum exhibits a rotated semicircle (Fig. 2), indicating that both reactions are under a charge-transfer control. A general model for the red–ox reaction with one adsorbed species [42] and mass/charge transfer limitations [43] is shown in Fig. 3. The model consists of the solution resistance, R_s, which is in series with the constant phase element, Z_{CPE}, in parallel with the charge transfer resistance, R_{ct}, which in turn is in series with a parallel connection of the pseudocapacitance C_p and resistance R_p. Moreover, the impedance of the mass or vacancies transfer through the oxide film, Z_w, has also been included. This is general model, which contains too many parameters and the use of the total model cannot be statistically justified. However, in each particular case the statistical analysis was performed and a maximal number of parameters was determined.

The CPE in Fig. 3 may be connected with the interface metal/oxide and/or with the dielectric oxide capacitance; nonhomogeneity of the film could create the distribution of time constants. The values of parameter T in the passivation range are of the order of 20–40 $\mu F\,cm^{-2}\,s^{-\alpha}$ which are in the range of the double layer capacitances and lower than usual oxide layer capacitances. However, the presence of this element is observed in the total potential range from hydrogen to oxygen evolution.

At the potentials of HER and OER, the films conduct well ($Z_w = 0$) and pseudocapacitance is not observed. In this case, the faradaic impedance is reduced to a simple charge transfer resistance. For hydrogen evolution, $R_{ct} = 33\,\Omega\,cm^2$ at $E = -1.2$ V and, for oxygen evolution, $R_{ct} = 3.8 \times 10^4\,\Omega\,cm^2$ at $E = 0.85$ V, which is associated with the difference in the hydrogen and oxygen reaction kinetics. In these potential regions, both reactions are controlled by the charge transfer process only, without diffusional effects.

To investigate the dependence of the electrode impedance on the d.c. potential, the freshly polished electrode was initially polarized at −0.9 V for 60 s, and the potential was stepped up to −0.6 V. After

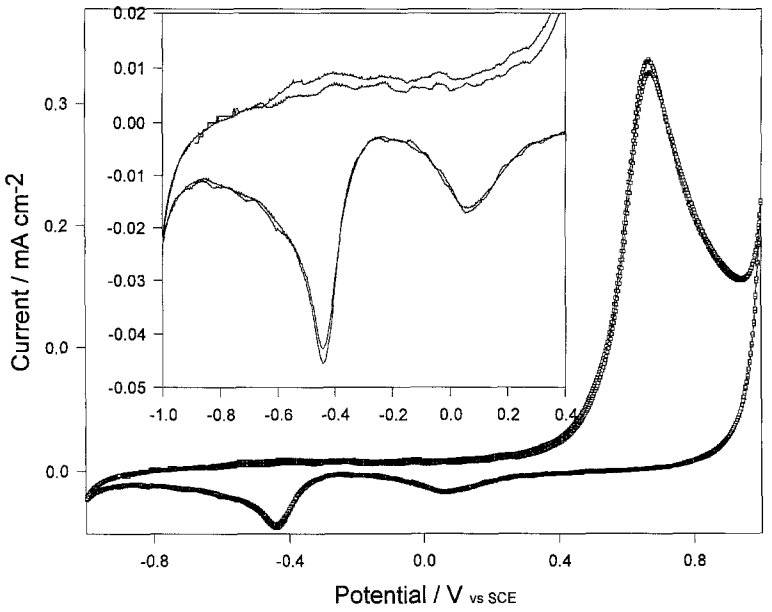

Fig. 1. Cyclic voltammogram for stainless steel 304 electrode ($A = 0.126\,cm^2$) rotated at 1000 rpm, $dE/dt = 0.02\,V\,s^{-1}$, in 1 M $NaHCO_3$ solution at pH 8 and at room temperature.

2 h of exposure, a steady-state current of a few $\mu A\,cm^{-2}$ was reached and the impedance was measured. Following the first set of impedance measurements, the potential was progressively raised in 100 mV steps to 0.8 V and the measurements were repeated after 2 h of polarization at a given potential. The surface film changed after the circuit was opened and the measurements were consequently performed at the constant anodic potentials. Figure 4 shows Nyquist diagrams corresponding to the impedance of the passive film at potentials ranging from −0.6 to 0.8 V; the points represent the measured data and solid lines are derived from simulations using the parameters summarized in Table 1. This representation was chosen to clearly show the effect of potential but the reliability of the equivalent circuit was also checked by Bode plots and the deconvolution method, in which the Warburg impedance contribution was subtracted from the total impedance spectra. The Bode plots were used because they are more sensitive to the presence of time constants.

The following features are noticed from the Nyquist plots in Fig. 4: (i) for a given frequency, the imaginary part $|Z''|$ is larger in the low potential region (−0.6 to 0.3 V) than in the high potential region (0.5 to 0.8 V); (ii) high R_{ct} values were observed for both potential ranges; (iii) the contribution of the Warburg diffusion impedance Z_w is large at low frequencies in both potential regions; (iv) a near-semicircular plot is observed at 0.4 V; the lowest values of $|Z''|$ and Z' are observed at this latter potential for any frequency value; (v) one time constant can be recognized for all

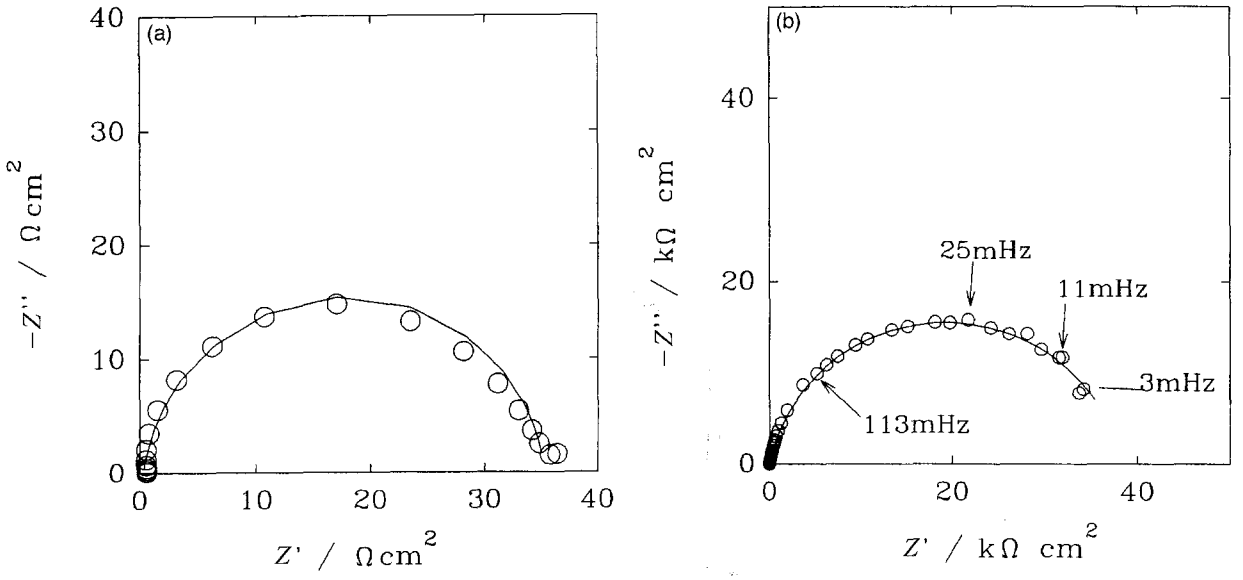

Fig. 2. Nyquist plots for the impedance data of the hydrogen evolution reaction at (a) −1.2 V and oxygen evolution reaction at (b) 0.85 V on a stainless steel 304 electrode ($A = 1\,cm^2$) rotated at 1000 rpm, in 1 M $NaHCO_3$ solution at pH 8. Points correspond to the data and solid lines display the fitting using the equivalent circuit of Fig. 3.

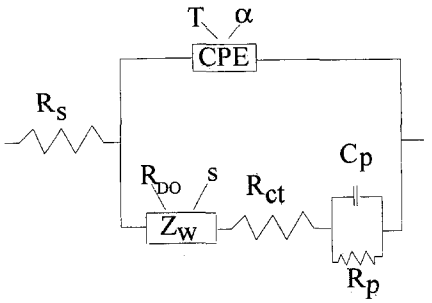

Fig. 3. Equivalent circuit used in analysing the impedance data of stainless steel 304 electrode.

potentials but two time constants were measured at 0.4 V and 0.5 V.

The log $|Z|$ against log f plots show an almost linear relation in medium frequency range with a slope about −0.9 and reveal that the high and low frequency extremes have slightly different slopes. The phase angle has values close to −90° in medium frequency range, but does not reach this value which corresponds to ideal capacitive behaviour [10–12]. The resistance at the high frequency limit corresponds to the ohmic resistance of the electrolyte, R_s, which always is about 1 Ω cm^2.

The impedance spectra in Fig. 4 (except for 0.4 V and 0.5 V) can be represented by a modified Randles equivalent circuit (Fig. 3), in which the faradaic impedance consists of the Warburg impedance, Z_w, and charge transfer impedance, R_{ct}. At these potentials, no fast changes of the surface coverage occur during the measurements and the pseudocapacitance may be neglected. The observed time-stability and reproducibility of the impedance spectra at constant potentials demonstrate that the passive film formation is irreversible process. The resistance corresponding to

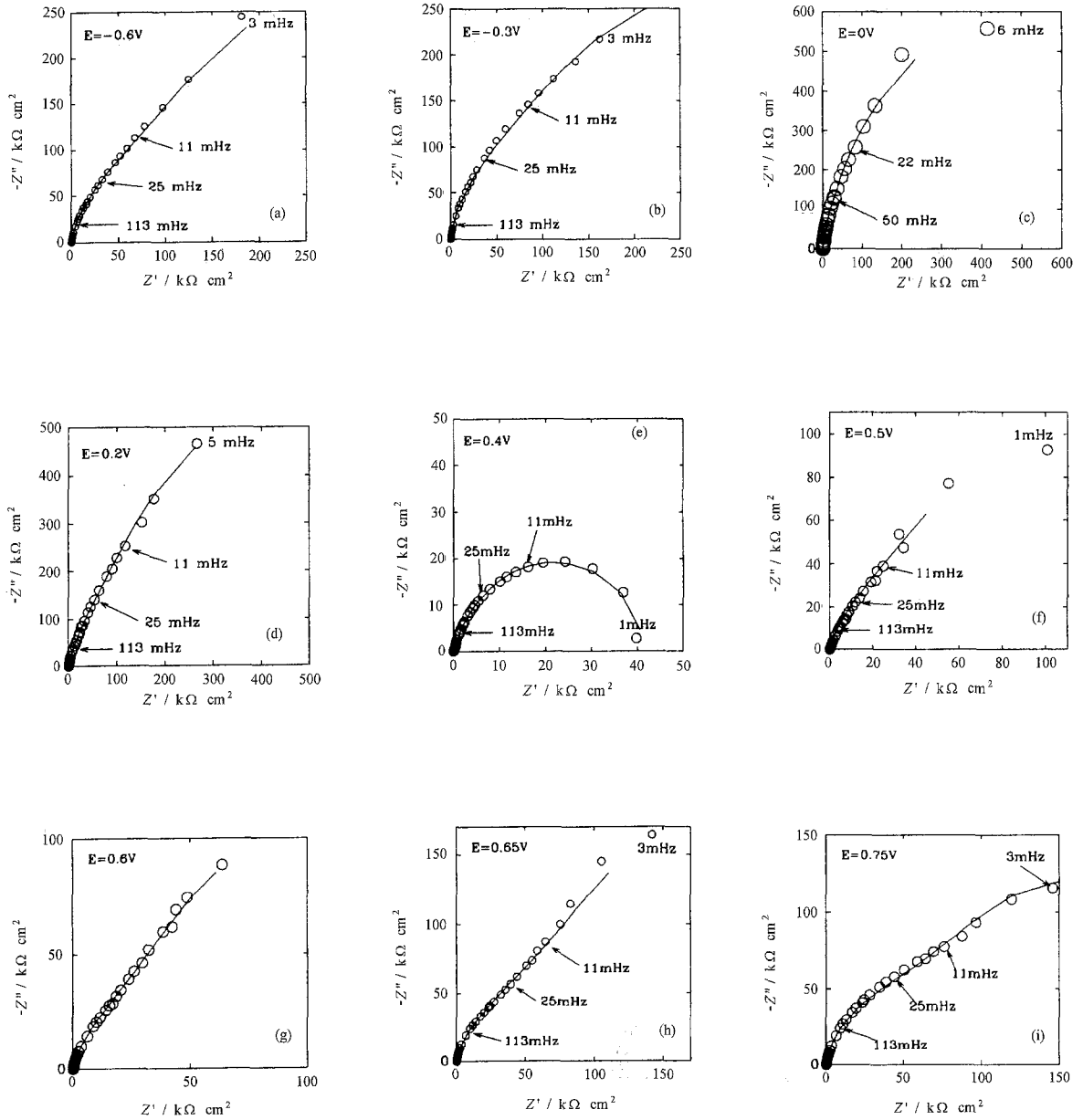

Fig. 4. Nyquist plots for the impedance data of anodic films formed after 2 h at increasing potentials on stainless steel 304 electrode (A = 1 cm^2) rotated at 1000 rpm, in 1 M $NaHCO_3$ solution at pH 8. The oxidation potentials as marked on diagrams. Points correspond to the data and solid lines display the fitting using the equivalent circuit of Fig. 3. Potentials, E: (a) −0.6, (b) −0.3, (c) 0, (d) 0.2, (e) 0.4, (f) 0.5, (g) 0.6, (h) 0.65 and (i) 0.75 V.

Table 1. Parameters for oxidation of SS304 electrode in 1 M $NaHCO_3$ solution at increasing oxidation potentials

Potential V vs SCE	*CPE paramater T* $\mu F\,cm^{-2}\,s^{-\alpha}$	*CPE parameter, α*	R_{DO} /kΩ cm²	l^2/D /s	R_{ct} /kΩ cm²	R_p /kΩ cm²	C_p /μF cm⁻²	C_{dl} /μF cm⁻²	*Slope dlog |Z| vs dlog ω*
−1.2	50.9	0.969	–	–	0.017			31	
−0.6	56.3	0.913	569	177	124				−0.895
−0.4	48.7	0.924	695	135	180				−0.920
−0.3	39.4	0.936	472	74	180				−0.923
−0.2	30.9	0.946	378	32	317				−0.936
−0.1	24.7	0.957	595	13	11				−0.949
0	20.2	0.972	1183	18	4.7				−0.960
0.1	20	0.969	2433	81	5.2				−0.953
0.2	23.6	0.965	126	102	1.7				−0.954
0.3	20	0.879	238	51	0.96				−0.852
0.4	29	0.998	3.8	7.4		37.1	498		−0.741
0.5	31	0.997	8.2	3.8		80.8	228		−0.813
0.6	53.2	0.925	256	76	20.3				−0.908
0.65	45.6	0.929	422	165	44.5				−0.915
0.7	43.6	0.921	576	425	56.6				−0.917
0.75	46.9	0.922	244	116	75.6				−0.906
0.8	62.7	0.908	164	127	95.8				−0.886
0.85	108	0.896			38			41	−0.876

low frequencies was very high, in agreement with the low corrosion rate. Since the impedance spectra obtained using the SS304 rotating disc electrode were independent of rotation speed, any diffusional resistance should lie within the oxide film of the electrode. This resistance is linked to the movement of ions/vacancies (possibly oxygen) through the surface layer, i.e. the diffusion of species through a finite region of length l corresponding to the thickness of the passive film. The finite Warburg impedance, Z_w, may be expressed [18] by the equation:

$$Z_w = R_{DO}(js)^{-0.5}\tanh(js)^{0.5} \qquad (2)$$

where $s = l^2(\omega/D)$, D being the diffusion coefficient of diffusing species in a passive film and $\omega = 2\pi f$. The diffusion resistance, R_{DO}, is the limit of $Z_w(\omega)$ for $\omega \to 0$ and may represent the resistance of mass transfer ions, defects or atomic oxygen through the surface film.

The impedance spectra are dominated by the Warburg impedance and the measurements have to be extended to low frequencies, since the significant experimental points are between 100 Hz and 1 mHz. The importance of Z_w in the total impedance is evidenced by subtracting the Warburg impedance from the impedance spectrum that led to the semicircle, as shown by the diagrams in Fig. 5 for the complex plane plots at −0.3 V and 0.75 V. The deconvolution method by eliminating the Warburg contribution Z_w from the measured data was also a good means of verifying the fitting parameters.

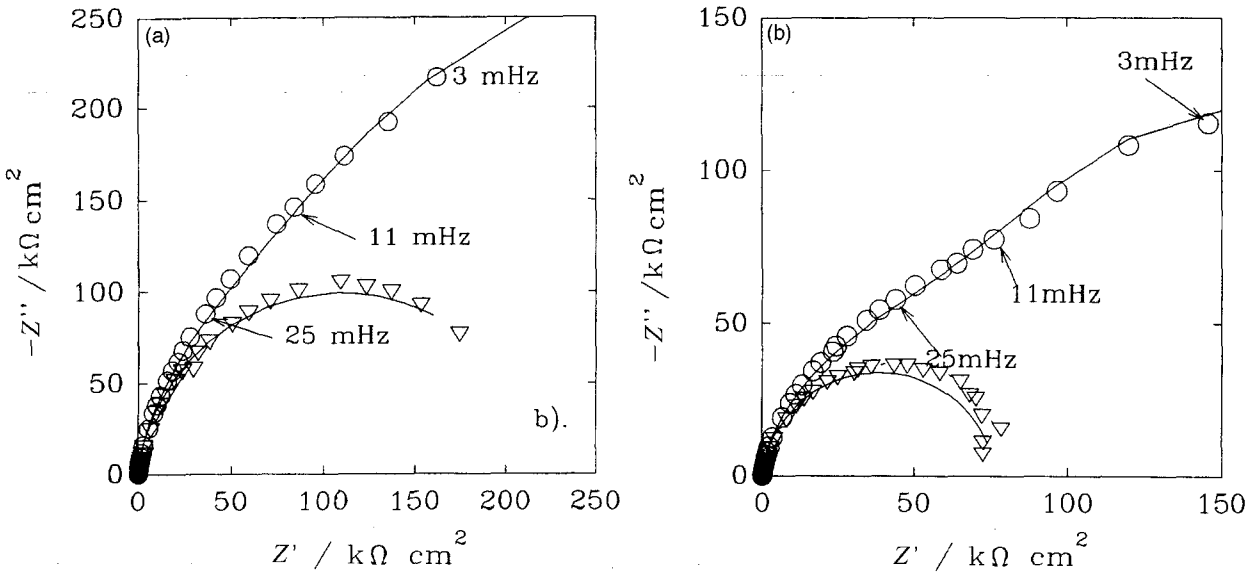

Fig. 5. Nyquist plots for the impedance data of anodic film formed after 2 h at applied d.c. potentials on stainless steel 304 electrode (A = 1 cm²) before (○) and after deconvolution (▽) by subtraction of the Warburg impedance contribution. The electrode rotated at 1000 rpm, in 1 M $NaHCO_3$ solution at pH 8. Points show the measured data and solid lines display the fitting using the equivalent circuit of Fig. 3. Potentials, E: (a) −0.3 and (b) 0.75 V.

The finite length diffusing element used here should give only real impedance at infinitely low frequencies. However, experimentally it was not possible to go to so low frequencies (our limit was 0.001 Hz). Because only initial part of the skewed semicircle was observed experimentally, the parameters R_{DO} and l^2/D could not be determined precisely. In fact, the values given in Table 1 and 2 lead to too small thickness. However, the presence of this element is statistically justified.

The charge transfer resistance, R_{ct}, increases with the applied potential and reaches its highest values between −0.4 V and −0.2 V (Fig. 6); it is connected with the film passivity. The decrease of R_{ct} in the potential range from 0 to 0.3 V indicates a beginning of film dissolution. The low R_{ct} value in the hydrogen evolution range clearly shows that the surface film is

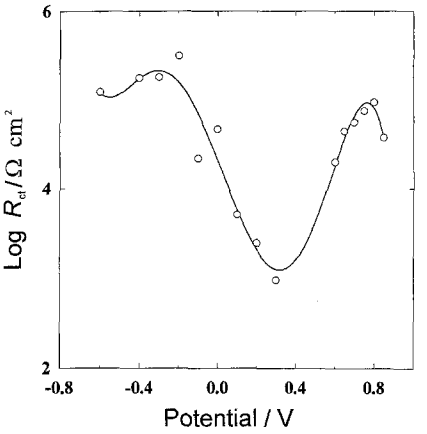

Fig. 6. Values of log R_{ct} as a function of anodic potential.

Table 2. Fitting parameters for SS304 electrode in 1 M $NaHCO_3$ solution at different potentials and oxidation times

Potential /V vs SCE	*Time* /h	*CPE parameter T* /μF cm^{-2} s$^{-\alpha}$	*CPE parameter α*	R_{DO} /kΩ cm^2	l^2/D /s	R_{ct} /kΩ cm^2	R_p /kΩ cm^2	C_p /μF cm^{-2}	*Slope log |Z| vs log ω*
−0.5	2	82.5	0.909	175	31	222			−0.909
	20	85	0.890	530	53	568			−0.901
−0.3	2	43.2	0.952	221	5.9	18			−0.944
	20	36.8	0.970	778	17.8	79			−0.956
−0.2	2	29.6	0.980	238	7.46	12			−0.943
	20	27.5	0.979	722	16.1	73			−0.951
−0.1	2	24.5	0.980	269	12	21			−0.958
	20	24.8	0.971	1159	14.6	474			−0.960
	44	22.1	0.974	4580	68	1250			−0.963
0	2	17.6	0.990	150	3.2	130			−0.950
	20	19.7	0.975	2710	33.7	215			−0.960
	92	39.0	0.971	9000	147	370			−0.957
0.1	2	19.3	0.973	464	24	1.1			−0.952
	20	22.9	0.949	1080	34	3.2			−0.927
	44	25.4	0.941	2108	161	2.7			−0.926
0.2	2	23.8	0.947	1423	111	1.2			−0.940
	20	28.0	0.933	1340	192	129			−0.923
	44	32.6	0.922	1610	367	171			−0.915
0.3	2	28.1	0.942	353	22.5	1.25			−0.873
	20	18	0.996	8.0	11.2		404	140	−0.836; −0.886
	44	24	0.998	10	13.8		280	256	−0.837; 0.856
	120	32	0.992	0.7	51		76	551	−0.815; 0.885
0.4	2	18	0.998	3.8	7.3		37	498	−0.881
	20	33.2	0.998	3.64	2.6		23	286	−0.827; −0.782
0.5	2	22	0.998	54	1.0		53	49	−0.813
	20	38	0.998	3.0	3.4		59	183	−0.820; −0.871
	68	38	0.997	4.3	0.8		57	58	−0.893
	92	36.5	0.997	4.16	0.8		85	51	−0.902
0.6	2	32.5	0.941	287	13	2.18			−0.918
	20	14.5	0.998	2.04	0.14		698	131	−0.865; −0.915
	40	13.7	0.997	2.45	0.12		605	180	−0.886; −0.907
	64	12.6	0.998	2.68	0.15		492	230	−0.865; −0.895
0.7	2	26	0.925	1430	163	157			−0.912
	20	30.6	0.887	968	67	68.2			−0.873
	44	26	0.926	1588	254	2.25			−0.877
	116	24.4	0.941	1240	153	3.61			−0.888
	120	26	0.930	1670	209	3.22			−0.883
	140	25.3	0.941	1580	196	3.61			−0.884
0.8	2	38.5	0.919	185	12	123			−0.907
	20	52	0.933	170	9.6	77.6			−0.892
	40	33.5	0.998	1.45	2.9		120	228	−0.715; −0.88
	116	36.6	0.997	3.59	5.9		162	286	−0.761; −0.869

thin and well conducting. Disappearance of R_{ct} and appearance of parameters R_p and C_p between 0.4 V and 0.5 V is in agreement with the observation of active dissolution. Such elements (pseudocapacitance) [44] appear when the surface coverage is changing with potential. The values of parameter T are relatively constant at 20 to 50 $\mu F\,cm^{-2}$ except at very positive potential. Besides, the parameter α is also between 0.9 and 1 which indicates that deviation from purely capacitive behaviour is relatively small. Its use, however, improves the approximation significantly what is confirmed by the sequential F-test.

The minimum values of Z_w and the slope d log $|Z|$/d log f (Fig.7) observed at 0.4 V are consistent with the thinning of the film ascribed to its partial dissolution. The Bode phase angle plots at 0.4 V (Fig. 8) and 0.5 V are characterized by the minimum in medium frequency part, which indicates the presence of a second element with a different time constant. The resistance R_p in parallel connection with the capacitance C_p may describe the faradaic reaction, the oxidation of Cr(III) or Cr(VI), and its further dissolution. Electrode depassivation at 0.4 V was manifested by an increase in d.c. current on the voltammogram (Fig. 1) with no traces of localized corrosion. An abrupt change in the properties of passive films on stainless steel in neutral solutions at 0.4 V is reported in the literature [1, 23–36]. Since Fe_2O_3 is isostructural with Cr_2O_3, Fe(III) may easily be substituted by Cr(III) and subsequently Cr(III) oxidizes to Cr(VI). From thermodynamic considerations [37–40], at 0.4 V a sufficient overpotential exists for chromium oxidation and dissolution, and the ratio of Fe_2O_3 to Cr_2O_3 in the passive film should be larger as the applied potential and/or oxidation time increase. The critical potential marks the boundary between two types of passive films: at low potential, a Cr-rich passive film protects the surface while above 0.4 V Cr(III) oxidizes to Cr(VI), which dissolves into the solution and/or is retained in the stable mixed oxide films. The presence of Cr(VI) in the oxides of the passive film on Fe–Cr alloys [27–33] and AlCr alloys [34, 41] at high positive potentials was demonstrated using X-ray adsorption near edge spectroscopy (XANES) [27–29, 34, 41] and XPS [31–33] techniques.

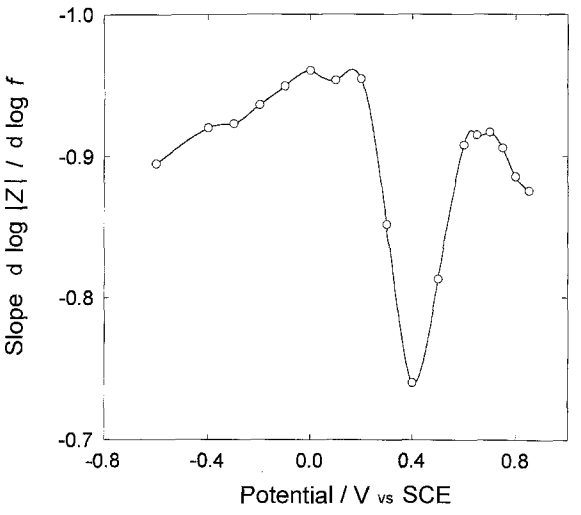

Fig. 7. Value of slope d log $|Z|$/d log f as a function of anodic potential. Slope values were calculated from the Bode magnitude plots of the impedance measured data against log frequency.

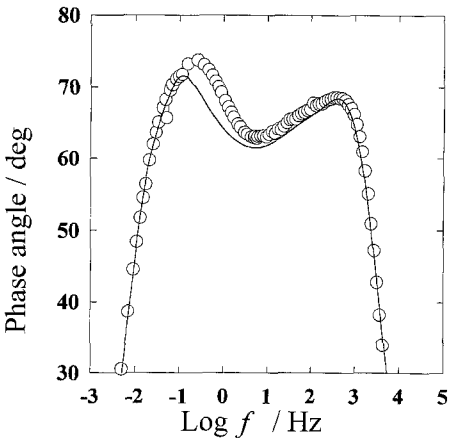

Fig. 8. Bode phase angle plot for impedance of anodic process at 0.4 V on SS304 electrode rotated at 1000 rpm in 1 M $NaHCO_3$ solution at pH 8. Points correspond to the data and solid line display the fitting using the equivalent circuit in Fig. 3.

The impedance spectra of a high potential passive film (0.6 V to 0.8 V) show the variation of parameters Z_w, R_{ct} and the slope d log$|Z|$/d log$f$ with the increasing potential, changes which support the idea of a new passive film being formed. Comparison of the parameters R_{ct}, slope d log $|Z|$/d log$f$ and Z_w calculated for impedance data in the low and high potential regions, using the same equivalent circuit suggests that a thicker and better conducting film is formed at higher potentials (> 0.5 V).

3.2. *Effect of oxidation time*

Measurements were carried out to investigate the changes in the passive film during polarization. A freshly polished electrode was first polarized at −0.9 V for 60 s, then kept at a given anodic potential. Impedance data were acquired first after 2 h of polarization and then the effect of longer polarization times was studied. The SS304 electrode was rotated at 1000 rpm and the 1 M $NaHCO_3$ solution was purged continuously with nitrogen gas. The parameters calculated from the analysis of the impedance spectra are summarized in Table 2. The effect of the exposure time on the parameters evidences a different behaviour of the passive film in the low and high potential regions.

The electrochemical characteristics of a passive film in the low potential region with one time constant are best described by the equivalent circuit with faradaic impedance consisting of R_{ct} and Z_w. Both Z_w parameters and the charge transfer resistance R_{ct}, steadily increase with the oxidation time, which suggests an improvement in the film passivity, while the oxidation rate, which is inversely proportional to R_{ct}, decreases with exposure time.

Two relaxation time constants were observed after several hours exposure at potentials ranging

from 0.3 V to 0.6 V and the impedance spectra were analysed using the equivalent circuit with Z_w in series with C_p in parallel connection with R_p. After an oxidation time longer than 20 h, a second time constant appears at low frequencies probably due to the oxidation–dissolution reaction, for example, Cr(III) to CrO_4^{2-} [37–40]. The values of parameters Z_w and R_p decrease with the polarization time. The simultaneous decrease of the resistances with the exposure time may be explained by the increase in the ionic conductivity through the passive film, indicating imperfect protective properties. The dependence of the resistances on the electrode potential and the oxidation time also indicates changes in the film composition with potential and exposure time. Morphological observations from electron microscopy do not show the precipitation of solid material but surface coloration to a uniform gold colour of the passive film could be seen with the naked eye. The coloration of passive film is associated with the optical phenomenon of multiple, thin layer beam interference [47]. The gold colour remained unchanged in air and in the solution under positive potential but disappeared at the open-circuit potential. The surface coloration confirms the film thickening at potentials above 0.6 V and the oxide reduction at potentials below 0.1 V.

4. Conclusions

The effects of oxidation potentials in the range from −0.6 to 0.85 V and an increasing exposure time on passive films formed on the surface of SS304 electrode were investigated by the impedance technique. Since the behaviour of the oxide film changes after the opening of the circuit, the measurements were performed at constant oxidation potentials.

The oxidation of an SS304 rotating electrode is controlled by both the charge transfer and the mass/vacancies transfer processes. The presence of the Warburg impedance is essential at each oxidation potential and the mass/vacancies transfer process is restricted by the infinite length of the surface film. The importance of the diffusion in the formation of a passive film is illustrated by subtracting the Warburg contribution from the measured impedance data.

The changes of impedance data indicate that the passive film formed in the low potential region is partially dissolved at 0.4 V and that, at higher potentials, a new passive film forms. Significant differences between the properties of low and high potential films are evidenced. Colouration of the SS304 electrode surface with the oxidation at high potentials proves the multiple thin layer formation and thickening of passive film. No traces of localized corrosion were detected.

Acknowledgements

This research was supported by Hydro-Québec (IREQ) and the Natural Sciences and Engineering Research Council of Canada.

References

[1] M. Drogowska, L. Brossard and H. Ménard, *J. Appl. Electrochem.* **26** (1996) 217.
[2] C. Y. Chao, L. F. Lin and D. D. Macdonald, *J. Electrochem. Soc.* **129** (1982) 1874.
[3] J. Bardwell and M. C. H. McKubre, *Electrochim. Acta* **36** (1991) 647.
[4] F. E. Varela, L. M. Gassa and J. R. Vilche, *J. Electroanal. Chem.* **353** (1993) 147.
[5] N. Benzekri, R. Carranza, M. Keddam and H. Takenouti, *Corros. Sci.* **31** (1990) 627.
[6] K. Noda, T. Tsuru and S. Haruyama, *ibid.* **31** (1990) 673.
[7] S. Turgoose and R. A. Cottis, *in* 'Electrochemical Impedance: Analysis and Interpretation', ASTM STP 1188 (edited by J. R. Scully, D. C. Silverman and M. W. Kending), American Society for Testing and Materials, Philadelphia (1993) pp. 173–91.
[8] C. Silverman, *ibid.* pp. 192-204.
[9] D. D. Macdonald and S. I. Smedley, *Electrochim. Acta* **35** (1990) 1949.
[10] F. Mansfeld and W. J. Lorenz, *in* 'Techniques for Characterization of Electrodes and Electrochemical Processes', (edited by R. Varma and J. R. Selman), J. Wiley & Sons, New York (1991).
[11] F. Mansfeld, *Electrochim. Acta* **35** (1990) 1533.
[12] F. Mansfeld, M.W. Kendig and S. Tsai, *Corrosion* **38** (1982) 478.
[13] G. W. Walter, *Corros. Sci.* **32** (1990) 1059, 1085.
[14] H. P. Hack and J. R. Scully, *J. Electrochem. Soc.* **138** (1991) 33.
[15] D. C. Silverman, *Corrosion* **47** (1991) 87.
[16] G. J. Brug, A. L. G. van den Eeden, M. Sluyters-Rehabach and J. H. Sluyters, *J. Electroanal. Chem.* **176** (1984) 275.
[17] A. Lasia and A. Rami, *ibid.* **294** (1990) 123.
[18] J. R. Macdonald and D. R. Franceschetti, *in* 'Impedance Spectroscopy, Emphasizing Solid Materials and Systems' (edited by J. R. Macdonald), J. Wiley & Sons, New York (1987).
[19] T. Pajkossy, *J. Electroanal. Chem.* **364** (1994) 111.
[20] A. Sakharova, L. Nyikos and Y. Pleskov, *Electrochim. Acta* **37** (1992) 973.
[21] K. Jüttner, *Electrochim. Acta* **35** (1990) 1501.
[22] J. R. Macdonald, J. Schoonman and A. P.Lehner, *J. Electroanal. Chem.* **35** (1990) 123.
[23] S. Silverman, G. Cragnolino and D. D. Macdonald, *J. Electrochem. Soc.* **129** (1982) 2419.
[24] A. Di Paola, *Electrochim. Acta* **34** (1989) 203; *Corros. Sci* **31** (1990) 739.
[25] P. Schmuki and H. Böhni, *in* Proceedings of the Symposium on 'Oxide Films on Metals and Alloys' (edited by B. R. MacDougal, R. S. Alwitt and T. A. Ramararayanan), The Electrochemical Society, Pennington, NJ (1992), p. 326; *J. Electrochem. Soc.* **139** (1992) 1908; *ibid.* **141** (1994) 362.
[26] N. Hara and K. Sugimoto, *J. Electrochem. Soc.* **126** (1979) 1328.
[27] J. A. Bardwell, G. I. Sproule, D. F. Mitchell, B. MacDougall and M. J. Graham, *J. Chem. Soc. Faraday Trans.* **87** (1991) 1011.
[28] J. A. Bardwell, G. I. Sproule, B. MacDougall, M. J. Graham, A. J. Davenport and H. S. Isaacs, *J. Electrochem. Soc.* **139** (1992) 371.
[29] A. J. Davenport, M. Sansone, J. A. Bardwell, A. J. Aldykiewicz, Jr., M. Taube and C. M. Vitus, *ibid.* **141** (1994) L6.
[30] G. G. Long, J. Kruger and D. Tanaka, *ibid.* **134** (1987) 264.
[31] A. R. Brooks, C. R. Clayton, K. Doss and Y. C. Lu, *ibid.* **133** (1986) 2459.
[32] C. R. Clayton and Y. C. Lu, *ibid.* **133** (1986) 2465.
[33] C. Calinski and H.-H. Strehblow, *ibid.* **136** (1989) 1328.
[34] A. J. Davenport, H. S. Isaacs, G. S. Frankel, A. G. Schrott, C.V. Jahnes and M. A. Russak, *ibid.* **138** (1991) 337.
[35] W. P. Yang, D. Costa and P. Marcus, *in* Proceedings, *op. cit.* [25], p. 516.
[36] D. Landolt, *in* 'Passivity of Metals' (edited by R. P. Frankenthal and J. Kruger), The Electrochem. Society, Princeton, NJ (1978), p. 484.
[37] E. Deltombe and M. Pourbaix, 'Compartement électrochimique du fer en solution carbonique, diagrammes

d'équilibre tension–pH du système Fe–CO_2–H_2O, à 25°C', CEBELCOR, Rapport technique no. 8 (1954).
[38] M. Pourbaix, 'Atlas of Electrochemical Equilibria in Aqueous Solutions', NACE, Texas (1974).
[39] K. Niki, *in* 'Standard Potentials in Aqueous Solutions' (edited by A. J. Bard, R. Parsons and J. Jordan), Dekker, New York (1985), p. 435.
[40] G. H. Kelsall, C. I. House and F. P. Gudyanga, *J. Electroanal. Chem.* **244** (1988) 179.
[41] G. S. Frankel, A. G. Schrott, A. J. Davenport, H. S. Isaacs, C. V. Jahnes and M. A. Russak, *J. Electrochem. Soc.* **141** (1994) 83.
[42] C. N. Cao, *Electrochim. Acta* **35** (1990) 831.
[43] M. Sluyters-Rehbach and J. Sluyters, *in* 'Comprehensive Treatise of Electrochemistry', vol. 9 (edited by E. Yaeger, J. O'M. Bockris, B. E. Conway and S. Sarangapani) Plenum, New York (1984) p. 177.
[44] F. E. Varela, L. M. Gassa, J. R. Vilche, *J. Electroanal. Chem.* **353** (1993) 147.
[45] M. J. Esplandiu, E. M. Patrito and V. A. Macagno, *ibid.* **353** (1993) 161; *Electrochim. Acta* **40** (1995) 809.
[46] U. Rammelt and G. Reinhard, *Electrochim. Acta.* **40** (1995) 505.
[47] S. Tolansky, 'Multibeam Interference Microscopy of Metals', Academic Press, New York (1970).